# On the growth kinetics of the protective passive film of the Delhi iron pillar

**R. Balasubramaniam**

Department of Materials and Metallurgical Engineering, Indian Institute of Technology, Kanpur 208 016, India

**A kinetic model for the evolution of atmospheric rust on the Delhi iron pillar (DIP) has been presented. The model is based on the known nature and structure of rusts on DIP and other corrosion-resistant ancient Indian irons. The initial fast rate of corrosion is aided by the entrapped slag inclusions and this results in enrichment of P at the metal–scale interface. The presence of P at the metal–scale interface promotes protective film formation processes (catalytic formation of δ-FeOOH and phosphates), thereby reducing the corrosion rate. Growth rates have been roughly estimated for these two regions based on available DIP rust thickness measurements.**

THE corrosion resistance of the 1600-year-old Delhi iron pillar (DIP; Figure 1) is due to the formation of a protective passive film on the surface, which is capable of withstanding atmospheric corrosion[1]. Characterization of the oldest rust on the pillar revealed that it contained amorphous iron oxyhydroxides and magnetite, and crystalline phosphates. The amorphous oxyhydroxides identified were lepidocrocite (γ-FeOOH), goethite (α-FeOOH), misawite (δ-FeOOH) and magnetite ($Fe_{3-x}O_4$). The phosphate identified was iron hydrogen phosphate hydrate ($FePO_4 \cdot H_3PO_4 \cdot 4H_2O$) (ref. 2). In addition to the nature and constituents of the long-term atmospheric rust, the structural features of DIP rust have also been analysed[1]. The process of protective rust formation can be summarized as follows. In the initial stages, the rust comprises of lepidocrocite and goethite. These forms of rust do not offer excellent protection and therefore the rate of corrosion is still maintained on the higher side. Conversion of part of this rust to magnetite does result in lower corrosion rates. However, the cracks and pores in the rust allow for diffusion of oxygen and complementary corrosion reactions. Moreover, reduction of lepidocrocite also contributes to the corrosion mechanism in atmospheric rusting[3,4]. The first step in enhanced corrosion resistance of the DIP results from the catalytic formation of δ-FeOOH (ref. 1). This phase is amorphous in nature and forms as an adherent compact layer next to the metal–scale interface. Its formation is catalysed by the presence of phosphorus in the DIP. Upon its formation, the corrosion resistance enhances significantly because δ-FeOOH forms a barrier between the rust and the metal. Such a mechanism is operative in the corrosion resistance of Cu- and P-containing weathering steels[5,6]. A modified scheme has also been proposed for these steels based on long-term observations[7]. In the special case of DIP and in the general case of ancient Indian irons, the presence of significant amounts of P in the metal (> 0.1%) leads to further effects, which have a direct bearing on their corrosion resistance. Due to the initial corrosion of metal, there is enhancement of P at the metal–scale interface. This P reacts with moisture and conditions are created in the rust that are ideal for formation of phosphoric acid, which eventually leads to the precipitation of phosphates in the long term. There are several phosphate-formation reactions[8]. The nature and type of phosphate will depend upon exposure conditions[8]. The nature of phosphate can provide ideas, in a qualitative manner, about the time period of the rust. For example, the phosphate identified in the DIP rust was crystalline in nature[2] and therefore, this indicated the relatively old age of the rust, because the phosphates that precipitate initially are amorphous in nature[8]. The formation of phosphates is beneficial to the corrosion resistance, because of their inhibitive nature. Added benefits accrue when the phosphate forms as a continuous layer next to the metal. In case of alternate wetting and drying cycles, like those obtained in atmospheric corrosion, the amorphous phosphates can transform to crystalline modifications and in this process there is a large reduction in porosity in the phosphate[8]. This transformation results in excellent corrosion resistance

**Figure 1.** Corrosion-resistant Delhi iron pillar.

*For correspondence. (e-mail: bala@iitk.ac.in)

properties. The above scheme has been elaborately discussed elsewhere with respect to the DIP's excellent atmospheric corrosion resistance[1].

The aim of the present communication is to utilize the nature of DIP rust, supplemented by the nature of protective rust on other ancient Indian irons that have successfully withstood atmospheric corrosion, to propose a possible kinetic scheme of passive film growth. There are several useful applications for long-term corrosion prediction models. For example, the prediction of long-term corrosion behaviour of outermost iron containers for interim nuclear waste storage is critical. In this respect, archaeological analogues assist in proposing reasonable predictions and in validating the probable corrosion kinetics models.

The first scientist to address corrosion kinetics of the DIP was Hudson[9]. Steel coupons (2 inches by 2 inches in cross section and 0.125 inch thick) were exposed in the open air near the pillar and the losses in weight were recorded after the corrosion products had been removed. He measured the corrosion rates as 0.23 mpy (mils/yr where 1 mil = 0.001 inch = 25.4 μm) for the period 1950–51 and 0.17 mpy for the period 1951–52 (ref. 9). Therefore, he arrived at an average value of 0.20 mpy for the corrosion of steel coupons in the vicinity of the pillar in the early 1950s. The steel, incidentally, did not contain entrapped slag inclusions like the DIP and secondly, contained 0.28% Cu. The beneficial effect of Cu on weathering resistance is now well understood – it catalyses the formation of protective oxyhydroxide δ-FeOOH as a continuous layer next to the metal–scale interface[5,6]. Assuming that the thickness loss was achieved uniformly from both sides of the exposed coupon, the average corrosion rate on each face is 0.1 mpy. Lahiri *et al.*[10] exposed a small piece (exposed area 4 $cm^2$ and 4.46 g in weight) of iron taken from the DIP to the industrial atmosphere of Jamshedpur and determined the atmospheric corrosion rate after 3.5 years exposure to be 0.261 mpy. Wranglen[11] assumed that the protective oxide formed was magnetite and co-related the corrosion rate, estimated by Hudson[9], to film thickness from the known densities of magnetite and iron. He thus estimated that the rust on DIP grew to 0.2 mil in one year. The densities of several oxyhydroxides of iron are presented in Table 1.

**Table 1.** Density of iron oxides and oxyhydroxides

| Name | Compound | Density (g/cc) |
|---|---|---|
| Wüstite | FeO | 5.7 |
| Hematite | α-$Fe_2O_3$ | 5.3 |
| Magnetite | $Fe_3O_4$ | 5.1 ~ 5.2 |
| Maghmite | γ-$Fe_2O_3$ | 4.9 |
| Goethite | α-FeOOH | 3.3–4.3 |
| Lepidocrocite | γ-FeOOH | 4 |
| Akaganeite | β-FeOOH | 3 |

The oxyhydroxides have different densities and therefore the estimated film thickness will depend upon the oxyhydroxide assumed to be formed. Difference in the densities between the dry and hydrated oxides (goethite, akaganeite and lepidocrocite) can also be noted. Therefore the estimated film thickness, based on magnetite formation, is a lower-bound value because the lower densities of the hydrated oxyhydroxides would have provided higher film thickness.

Applying parabolic kinetic law to depict protective growth of film (i.e. $y^2 = k_p t$ where $y$ is the thickness, $t$ the time and $k_p$ the parabolic rate constant), the parabolic constant, based on Hudson's data, can be estimated as 0.04 $mils^2/y$. Wranglen[11] extrapolated the data to 1600 years utilizing the parabolic rate law and calculated the anticipated film thickness as 8 mils. This is much lower than the DIP's rust thickness determined experimentally by Bardgett and Stanners[12], although Wranglen mentioned that his estimate was in agreement with the thickness measurements. It has, therefore, been reasoned that the relatively low humidity levels of Delhi were responsible for the pillar's excellent corrosion resistance, because the mild steel coupon corroded at a low rate[9,11].

Bardgett and Stanners[12], utilizing the corrosion rate data of Hudson (0.20 mpy) and assuming linear corrosion kinetics, stated that the surface must have corroded to (1600 years × 0.2 mils/year =) 320 mils per two faces. They did not apply the correction for corrosion occurring on two faces of Hudson's test specimen. Applying this correction, the corrosion thickness loss is 160 mils per face. They stated that the presence of Cu in Hudson's steel sample would have lowered the corrosion rate when compared with that of ordinary mild steel, and applied a correction factor of 1.2 to account for the absence of Cu in DIP[12]. This provides a corrosion loss of 192 mils per face for 1600 years of exposure. They applied further corrections to account for the lowering of atmospheric corrosion rate with time, and arrived at an average total corrosion loss to be 150 mils during the life of the pillar. Assuming the conversion of this corroded iron to magnetite, the estimated thickness of the surface film is approximately 300 mils. The degree of corrosion was also estimated by Choudhury to be 329 mils (ref. 13). It can be noted that he has applied a linear rate of corrosion based on Hudson's data to arrive at this estimated value. Based on this estimate, Choudhury mentioned that the total corroded portion of the surface of the pillar above the ground must be 500 kg and concluded rightly that actual corrosion to this amount did not occur. A close-up view of the oldest Sanskrit inscription (Figure 2) clearly shows that corrosion to this magnitude has not occurred.

There are several criticisms regarding the application of these models. First, the assumption that a unique corrosion process is operative throughout, is incorrect. Secondly, the assumption of magnetite as the corrosion product to model film thickness is not appropriate.

Thirdly, the extrapolation of corrosion rates determined utilizing small coupons[9,10] to the large mass of the pillar (approximate weight 6000 kg and exposed surface area 18000 $cm^2$; (ref. 14)) may be fraught with errors because of the mass metal effect[12]. The process of rust formation on the DIP is better-understood now[1,2] and therefore, the nature and constituents of the rust need to be taken into account in the model. It can be anticipated that the rust thickness must be high in the initial stages of rust formation due to the lower densities of the hydrated oxyhydroxides. Once the protective oxide (δ-FeOOH) forms, the rate is lowered. The formation of a phosphate layer would further reduce the rate. Alternate wetting and drying conditions lead to the formation of crystalline phosphates (thereby reducing drastically the porosity levels in the phosphate) and this results in further lowering of rates. Therefore, the model for rusting of DIP must take into account the sequence of protective film growth on the pillar.

In this context, visual observations on the rusting of DIP will be discussed. The observations of Ghosh[13] on the rusting of a freshly cut surface of the DIP provide insights on the initial film formation conditions. He stated that in one year's time after the surface was freshly cut some brown oxide could be removed by rubbing, but an adherent thin layer of rust was formed, though very thin and unequally distributed. The oxyhydroxides of iron are brownish in colour, while magnetite is black in colour[7]. After 14 months a thin film was formed, but again it was not uniformly distributed. In another six months (i.e. total of 20 months), the colour of the film was almost the colour of the main surface and the film was still thin and non-uniformly distributed. The rust was still bright at some places and also rusting pits were found, some of which could be removed by rubbing. At this point, the surface was rubbed with emery paper to remove the rust which came off under slight rubbing. The pits remained. After another 15 months of this rubbing exercise, the surface was observed. The pits had smoothed out, excepting one or two, but the location was still bright and had not taken the colour of the nearby surface. The above studies clearly indicate that the formation of the surface film on a freshly-cut surface of DIP is time-dependent.

Ideas about the film formation were also obtained from the colour of the growing rust on the DIP[15]. The Archaeological Survey of India (ASI) has constructed an iron grill cage (Figure 1; see also cover page of *Current Science*, 1997, **73**) surrounding the DIP in 1997 to prevent visitors from touching and damaging the pillar. The lower surface of the pillar above the ground, before the iron grill

**Figure 2.** Close-up view of the oldest Sanskrit inscription showing minimal corrosion damage.

**Figure 3.** Lower surface of the pillar above the ground, before the iron grill cage was constructed, revealed three distinct regions: the lowermost rough portion of the pillar, the smooth region that appears just above the rough portion and the polished surface that appears very bright.

cage was constructed (Figure 3), revealed three distinct regions – the lowermost rough portion of the pillar (that was used for the gripping of the pillar to the ground when it was originally buried in the temple), the smooth region that appears just above the rough portion (which is due to the habit of people encircling their hand before the stone platform was constructed in the last century by Beglar) and finally, the metallurgically polished surface that appears very bright (which was due to the habit of people encircling the pillar with their hands). The surface of the smoothly-polished region was photographed at periodic intervals after the construction of the grill cage to obtain insights on rust formation at this location. Presence of a rectangular metal insert at the polished region provided a convenient reference frame (Figure 4 *a*). After about a year of construction of the cage, the following observations were made. The polished surface was covered with a thin adherent layer of dark-brown rust which was adherent on the surface (Figure 4 *b*). In the location of some of the forge-welded joints the rust was black in colour, indicative of rough surface regions (thereby resulting in poor reflectivity) in these areas of enhanced corrosion caused by the presence of the interface. The bottom regions of the pillar generally showed evidences for significantly enhanced corrosion after one year of construction of the cage[15]. The growing rust must be composed of γ-FeOOH, α-FeOOH and magnetite in addition to amorphous oxyhydroxides[1,2]. It must be noted that some of the individual iron lumps that were used for manufacturing the pillar (by forge welding) have been delineated due to the rusting process. This region appeared almost similar to the rest of the surface of the pillar approximately three years after the construction of the cage (Figure 4 *c*). It must be noted that the film thickness must be relatively small, as the surface possessed good reflectivity.

Figure 5 *a* shows the rust on the previously brightly polished region approximately three years after construction of the iron cage (photographed in February 2000). The rectangular insert again provides a convenient reference point. It can be noticed that the protective passive film has nearly covered the previously brightly polished surface. Moreover, the colour of the passive film is relatively darker and appears similar to the colour of the surface in the rest of the pillar. The reason for the darker hue is because the photograph was recorded early in the morning. The same region, when observed in morning sunlight (photographed in August 2000; Figure 5 *b*) or in bright sunlight (photographed in February 2001; Figure 5 *c*) has a colour similar to that of the upper regions of the pillar. During the observations in February 2001, at least five locations with greasy patches (each extending completely around the full circumference of the pillar) were observed (Figure 1)[16]. Several large permanent red-coloured markings, in addition to these greasy patches, were also observed (Figure 6 *a*)[16]. The greasy patches have been apparently removed by surface cleaning using acetone in March 2001. When the pillar was studied in October 2001, several new prominent white, painted patches and oil streaks were observed on the surface (Figure 6 *b*).

The colour of the stable protective film that forms on the pillar after long exposure in the environment, is also briefly addressed. Some early observers of the pillar (in the 19th century AD) have stated that it possessed a

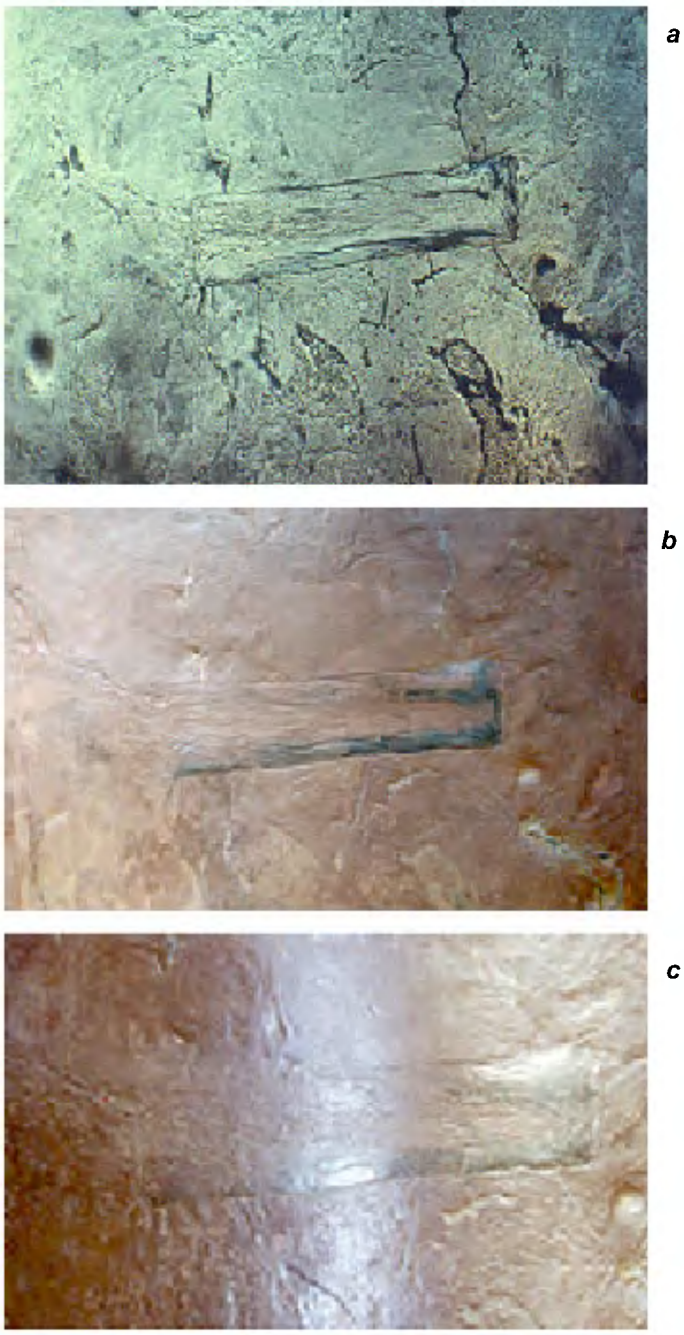


**Figure 4.** Structure of the pillar in (***a***) the polished region before construction of the iron grill cage. The previously polished surface after (***b***) one year (photographed in December 1998) and (***c***) three years (photographed in August 2000) after construction of the grill cage.

golden hue[17]. When the DIP is viewed normally, it appears black in colour with good reflectivity[15], indicating that the passive layer is relatively thin. However, when the DIP surface (especially the region inaccessible earlier to the public, i.e. above the oldest Sanskrit inscriptions) is viewed at an acute angle in bright sunlight, the colour of rust is yellowish-red in nature, and it provides the visual effect of a golden hue. Interestingly, yellow specks can be seen distributed all over the rust layer; this must be the crystalline phosphate. Therefore, the golden hue of the pillar is related to the protective passive film that forms on its surface.

A significant conclusion of the visual observations is that a polished surface attains a colour similar to that of the rest of the pillar surface in a time period of approximately three years. This is an important time in the protective film formation. Therefore, modelling of the protective film growth should account for at least two district regions – an initial period of fast rust formation and the second period, wherein the corrosion rate is drastically reduced due to modifications in the atmospheric rust.

Atmospheric corrosion damage is measured either by the mass loss per unit area or by average penetration depth, both of which can be related to the scale thickness. The generalized form of corrosion damage is given by[18–20]

$$y = kt^n. \quad (1)$$

As long as a unique rate law is obeyed, atmospheric corrosion data will fall on straight lines when plotted on logarithmic scales. The straight line relationship is given by

$$\log y = \log k + n \log t. \quad (2)$$

The term $k$ is generally a measure of the reactivity of the material with the environment and $n$ provides a measure of the protective ability of the corrosion product(s). In the case of linear rate law, $n = 1$ and $k$ is termed as the linear rate constant ($k_l$); and when $n = 0.5$, the parabolic rate law is obeyed and $k$ is called the parabolic rate constant ($k_p$). In the above law, the exponent $n$ usually varies between 0.5 (parabolic rate law) and 1.0 (linear rate law) for several metals and alloys (carbon and low alloy steels, galvanized steel, copper, copper alloys, etc.) in a wide variety of atmospheric environments[20]. In case of non-protective film formation, the corrosion rate depends upon the supply of the corrodents and moisture to the surface, and a linear rate is observed ($n = 1$). Such a linear rate has been experimentally observed in the initial stages of atmospheric corrosion for a wide variety of materials (low alloy steels, non-ferrous metals, zinc-coated steels, aluminum-coated steels, etc.)[18,21–23]. The formation of more resistant corrosion products results in protective film formation, and the atmospheric corrosion rate is then dictated by the diffusion of ions through the protective film. In such cases, the parabolic rate law is


**Figure 5.** Appearance of the polished region photographed in (***a***) early morning light (February 2000), (***b***) morning sunlight (August 2000) and (*c*) bright sunlight (February 2001).

obeyed ($n = 0.5$). In the overall sequence of atmospheric corrosion for several metals and alloys, the formation of corrosion-resistant products from repeated wet–dry cycling results in increasing protective ability with exposure time[20].

The process of protective film formation on DIP clearly indicates that the iron corrodes at a very fast rate initially and then at an extremely low rate[1]. Interestingly, the faster corrosion rate in the initial stages is aided by the presence of entrapped slag inclusions in DIP, and hence they indirectly promote passivation by causing enrichment of P at the metal–scale interface[1] and by altering the polarization characteristics[24]. The variation of DIP rust thickness with time is proposed to occur as depicted in Figure 7. The kinetic data presented in Figure 7 are based on the results of Bardgett and Stanners[12], coupled with the known observations of film formation on DIP. The kinetic data analysis has been described in detail later. Two district regions can be identified. A region in the initial period in which the film thickness grows rather rapidly, and a second region where the thickness increases by a small amount. Micromechanical models are also available, that provide details of the reduction and oxidation reactions in each wet and dry cycle[25]. The micromechanical models of rust growth (taking into account the composition, porosity, tortuosity of pores, specific area of rust, etc.) deal with rusting over a time horizon of each wet and dry cycle (i.e. over a period of a day). On the other hand, the macroscopic rusting model (Figure 7) addresses kinetics of scale growth over a much longer time horizon. The macroscopic model described above is compatible with the micromodels of rust growth over shorter periods of time (for example, linear growth models for the initial stage).

The initial period corresponds to the formation and growth of the non-protective oxyhydroxides and hence a linear rate of corrosion has been assigned for the initial region. It is reasonable to assume a linear rate because the oxyhydroxides that initially form on the surface of iron do not prevent the ingress of oxygen and moisture through the film to the metal surface[18,21]. Oxygen reduction readily occurs, thereby supporting the metal corrosion reactions. Reduction of γ-FeOOH (the first corrosion product to form) will also aid the corrosion reaction[3,4].

The second region in the kinetic schematic (Figure 7) corresponds to protective film formation. In the following discussion, the changes in this protective film will not be addressed. Nevertheless, it is known that there are at least three mechanisms resulting in protectiveness in the case of DIP; namely, δ-FeOOH formation, amorphous phosphate layer formation and finally crystalline phosphate layer formation[1]. All these processes are clubbed


**Figure 6.** ***a***, Several greasy patches (extending completely around the full circumference of the pillar) and several large permanent red-coloured markings were observed in February 2001 (ref. 16). These have been apparently removed by surface cleaning with acetone in March 2001; ***b***, One of the new, white painted patches and many oil streaks observed on the surface, when the pillar was studied in October 2001.

under the general regime of protective passive film growth in the following discussion. As visual observations of rusting on DIP showed that the protective film growth begins approximately at the end of three years and continues to provide corrosion resistance, the growth of only this film will be considered after the three-year initial period. Parabolic kinetics would apply to the second region because diffusional growth of the protective layer is best described by this law. It must be noted that logarithmic rate law cannot be utilized for modelling the second region. The logarithmic ($y = k \log t$) or inverse logarithmic rate laws have been applied to analyse corrosion data for several materials *only* for atmospheric corrosion situations characterized by dry conditions (i.e. with the relative humidity levels never exceeding 50%). Mechanistically, the logarithmic rate laws describe the growth rate limited by the diffusion of ions under a strong electric field along the thin oxide film in non-aqueous environments[20]. Therefore, the logarithmic rate law can be applied only to corrosion products formed in the most benign atmospheric conditions, particularly dry environments. As the humidity level of Delhi is higher than 50% for significant periods in the year (nearly eight months from July to March[11]), the modelling of atmospheric corrosion of DIP by the logarithmic rate law is not valid.

The division of the kinetic regime into two distinct regions has strong experimental support based on observations of rust cross-sections of ancient Indian irons. The difference between amorphous and crystalline phases in the rust could be identified by their optical property; i.e. the crystalline phases appear bright, whereas the amorphous phases are optically dull[7]. A three-layered structure was predicted for the DIP rust and this was confirmed by the analysis[1] of published rust cross-sections[13]. The multi-layered DIP rust cross-section is shown in Figure 8 *a*. It has been described in detail elsewhere[1] that the outermost layer (labelled A in Figure

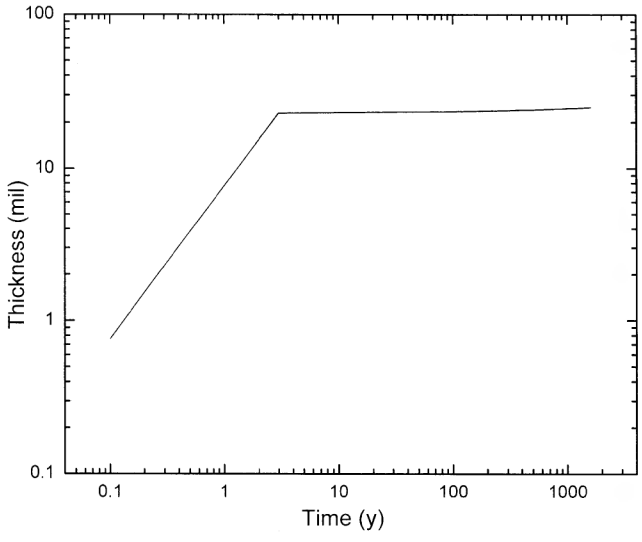


**Figure 7.** Proposed variation of rust thickness with time for the pillar indicating two distinct regions: One where the film thickness grows rapidly and another where thickness increases by small amounts.

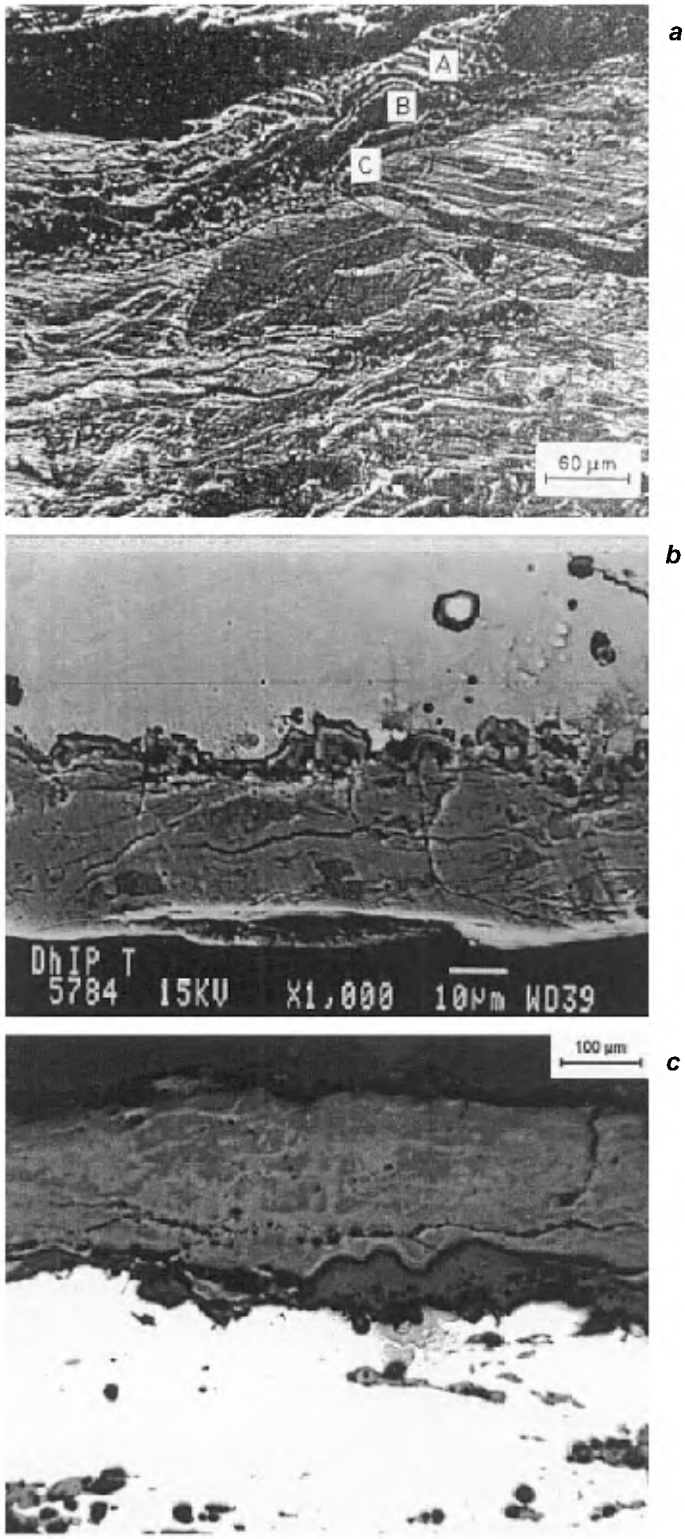


**Figure 8.** Multi-layered scales noticed in the rust cross-sections of (*a*) Delhi iron pillar, (*b*) Dhar iron pillar, and (*c*) iron clamp from the Gupta temple at Deogarh. (Photograph 8 *c* courtesy: P. Picardo).

8 *a*) contains the usual non-protective corrosion products, while the inner protective layers develop due to the presence of a significant amount of P in the metal (the middle layer, labelled B, being δ-FeOOH and the innermost layer adjacent to the metal, labelled C, being the phosphate layer). Fine details about this rust cross-section have been discussed in detail, elsewhere[1]. Unfortunately, the measurements from this cross-section (which was obtained from a sample extracted from the buried underground region[13]) cannot be utilized for modelling rusting of the DIP because the iron in the underground region is subjected to intense galvanic corrosion, due to the coating of lead on the pillar in the buried underground regions[26]. Unfortunately, repeated requests by scholars to replace this lead coating with another suitable coating has not yielded any results[17,26-28].

The multi-layered nature of atmospheric rust has also been observed in several other ancient Indian irons. For example, Figure 8 *b* provides the rust cross-section of iron from Dhar iron pillar, while Figure 8 *c* provides the cross-section of the atmospheric rust on an iron clamp from Deogarh. The Dhar iron pillar has been conservatively dated to 1050 AD (ref. 29), while the iron from the Deogarh temple has been conservatively assigned to the late-Gupta period of about 600 AD. The atmospheric rusts on these irons were clearly composed of an inner dull layer and an outer bright layer. A similar nature was also observed in the case of an ancient Indian iron clamp from the Gupta temple at Eran[30]. Based on optical properties[7], the inner layer has been considered to be amorphous in nature, and the external layer as crystalline. Analysis of phases and their distribution by microdiffraction and nuclear microprobe techniques has further revealed that the type (i.e. composition) and nature (i.e. crystalline or amorphous structure) of phase(s) identified near the interface depended upon the P concentration in the metal just below the scale[25] and there was a variation in phase distribution on profiling across the rust cross-section (ref. 31; Dillmann, P. and Balasubramaniam, R., unpublished work). Interestingly, ancient Indian iron invariably contained a significantly higher amount of P, the origin for which has been analysed in detail elsewhere[32]. The above examples illustrate the basis for modelling kinetics of rusting of DIP in terms of multi-layered rust growth.

Ideally, the thickness of the DIP rust layers obtained at several different locations on the pillar needs to be known in order to model passive film kinetics. The constituents and microstructure of the scale also need to be known, so that the kinetics can be related to the scale nature. Unfortunately, the microstructure of the rust cross-section in the exposed regions of the DIP is not available.

There is, however, one reported thickness measurement of the DIP rust by Bardgett and Stanners[12]. Using a permanent magnet thickness gauge, they obtained a thickness of less than 2 mils in the (previously) brightly polished part of the pillar and 20–25 mils in the rougher portion immediately above this (see Figure 3). They also reported that the readings were fairly constant around the circumference of the pillar. This indicates the uniform nature of the atmospheric corrosion product. From 6 feet above the base, and as high as could be reached, the scale thickness appeared smaller again[12]. They also mentioned that lower thickness readings would be given by the meter used by them on scales containing magnetic oxides of iron. This is the only available thickness measurement of the DIP rust.

Some kinetic data analysis can be performed using the results of Bardgett and Stanners[12], coupled with the known observation of the nature of film formation on the surface of DIP[1,13]. It is assumed that the thickness of the film in the parts that were accessible to the public is that of the adherent passive film, while the thickness in the region beyond public reach is assumed to be composed of both the protective and non-protective layers. The fracture and subsequent fall of the outer layer must be aided by the relatively porous nature of this film and by the internal defects like cracks and pores, which are frequently observed in the non-protective outer layers (see, for example, Figure 8 *b* and 8 *c*). Interestingly, studies on atmospheric rust of ancient Indian iron indicate that atmospheric film thickness in Indian iron was of the order of 20 to 40 mils (refs 29–31).

Once the protective passive film formed at the metal–scale interface, the diffusional transport of ions and oxygen/moisture would be greatly hindered due to its compact nature. The scale that forms in the initial stages of atmospheric rusting would remain in the outer regions of the rust. However, an important effect of long-term exposure on the outer non-protective film needs to be noted. The long-term atmospheric environmental exposure results in alternate wet and dry cycling of the rust and in this process, the constituents of the outer layer transform from a fine-grained structure to nanosized structure and finally to amorphous structure[1]. The amorphization of the oxyhydroxides of iron and magnetite in the atmospheric rust due to wetting and drying cycles has also been experimentally confirmed[33].

Relating the maximum measured thickness of Bardgett and Stanners[12] of 25 mils to the combined thickness of protective and non-protective rust, and the minimum measured thickness of 2 mils to the thickness of the protective rust, some numbers for the proposed growth kinetics can be obtained. The initial non-protective rust thickness is 23 mils because the protective layer thickness is assumed as 2 mils. If a linear rate of corrosion is assumed for the first three years ($y = k_1 t$), then the linear rate constant is estimated to be 7.67 mils/y. The corrosion rate predicted (i.e. 7.67 mils in the first year) is much higher compared to the estimations of Hudson[9] and Lahiri *et al.*[10] (Interestingly, the corrosion rates for a DIP sample of 0.24 $cm^2$ area was determined by immersion

testing to be 1.1 mpy in 0.001% NaCl solution and 9.9 mpy in 0.003% $SO_2$ solution[13].) However, such a high corrosion rate can be expected in the initial period because of the presence of entrapped slag particles in the matrix of DIP[1,24]. The role of entrapped slag inclusions on the corrosion behaviour of ancient Indian iron has been elucidated by the mixed potential theory[24], where the beneficial effect of slag inclusions in aiding passive film formation has been noted. The high rate of corrosion of Indian iron in the initial stages has been also confirmed by weight loss measurements by immersion testing of a Gupta-period iron from Eran[34]. Interestingly, after an initial period of high corrosion rate of ancient Indian iron, there was a drastic decrease in the rate with increasing time[34].

As regards the growth kinetics of the protective layer, its thickness after a period of approximately 1600 years is 2 mils, as discussed earlier. Assuming that this thickness has evolved over the remaining period (i.e. the only growth that took place was that of the inner protective film in the 1600 years of the pillar), the parabolic rate constant can be estimated as 0.0025 $mil^2$/yr. Therefore, it is proposed that the rate decreases drastically once the protective passive film forms at the metal–scale interface. The most important aspect in the above analysis is that the corrosion of the pillar virtually ceases once the protective film forms (Figure 7). It is interesting to note that the kinetic behaviour proposed is similar to the kinetics of corrosion of an active–passive metal when coupled to a cathodic material[35]. In this case, corrosion virtually ceases after an initial period of fast corrosion rate, which is due to the induction of passivity on galvanic coupling[34]. The similarities are quite significant with the major difference being that in the case of DIP, the galvanic coupling is with locations containing entrapped slags (for reasons discussed in detail, elsewhere[1]).

A kinetic model for the growth of the (protective and non-protective) rust on the DIP has been proposed based on the known nature and structure of the rust on DIP and other corrosion-resistant ancient Indian iron structures. The initial fast rate of corrosion is aided by the entrapped slag inclusions and this leads to enrichment of P at the metal–scale interface. The presence of P at the metal–scale interface promotes protective film formation processes (catalytic formation of δ-FeOOH and phosphates). Once the protective passive film forms on the surface at the metal–scale interface, the corrosion rate reduces drastically. Growth rates have been roughly estimated for these two regions based on available DIP rust thickness measurements.


1. Balasubramaniam, R., *Corros. Sci.*, 2000, **42**, 2103–2129.
2. Balasubramaniam, R. and Ramesh Kumar, A. V., *ibid*, 2000, **42**, 2085–2101.
3. Evans, U. R., *ibid,* 1969, **9**, 813–821.
4. Evans, U. R. and Taylor, C. A. J., *ibid*, 1972, **12**, 227–246.
5. Misawa, T., Kyuno, T., Suetaka, W. and Shimdaira, S., *ibid*, 1971, **11**, 35–48.
6. Misawa, T., Asami, K., Hashimoto, K. and Shimdaira, S., *ibid*, 1974, **14**, 279–289.
7. Yamashita, M., Miyuki, H., Matsuda, Y., Nagano, H. and Misawa, T., *ibid*, 1994, **36**, 283–299.
8. Ghali, E. L. and Potoin, R. J. A., *ibid*, 1972, **12**, 583–594.
9. Hudson, J. C., *Nature*, 1953, **172**, 499–500.
10. Lahiri, A. K., Banerjee, T. and Nijhawan, B. R., *NML Tech. J.*, 1963, **5**, 46–54.
11. Wranglen, G., *Corros. Sci.*, 1970, **10**, 761–770.
12. Bardgett, W. E. and Stanners, J. F., *J. Iron Steel Inst.*, 1963, **210**, 3–10; *NML Tech. J.*, 1963, **5**, 24–30.
13. Ghosh, M. K., *NML Tech. J.*, 1963, **5**, 31–45.
14. Balasubramaniam, R., *Curr. Sci.*, 1997, **73**, 1057–1067.
15. Balasubramaniam, R., *Bull. Met. Mus.*, 2001, **34**, 64–86.
16. *Times of India*, 19 March 2001.
17. Balasubramaniam, R., *Delhi Iron Pillar: New Insights*, Indian Institute of Advanced Study, Shimla and Aryan Books International, New Delhi, 2002.
18. Knotková-Čermáková, D., Vlcková, J. and Honzák, J., in *Atmospheric Corrosion* (eds Dean, S. W. and Rhea, E. C.), American Society for Testing and Materials, Philadelphia, ASTM STP 767, 1982, pp. 7–44.
19. Pourbaix, M., in *Atmospheric Corrosion* (ed. Ailor, W. H.), John Wiley, New York, 1982, pp. 107–121.
20. Leygraf, C. and Graedel, T. E., *Atmospheric Corrosion*, Wiley-Interscience, New York, 2000, pp. 101–103.
21. Horton, J. B., Ph D dissertation, Lehigh University, Bethlehem, USA, 1964.
22. Legault, R. A. and Pearson, V. P., *Corrosion*, 1978, **34**, 433.
23. Legault, R. A. and Pearson, V. P., *ibid*, 1978, **34**, 344.
24. Balasubramaniam, R., *NML Tech. J.*, 1995, **37**, 123–145.
25. Stratmann, M., Bohnenkamp, K. and Engell, H.-J., *Corros. Sci.*, 1983, **23**, 969–985.
26. Balasubramaniam, R., *Curr. Sci.*, 1999, **77**, 681–686.
27. Lal, B. B., in *The Delhi Iron Pillar: Its Art, Metallurgy and Inscriptions* (eds Joshi, M. C., Gupta, S. K. and Goyal Shankar), Kusumanjali Book World, Jodhpur, 1996, pp. 22–58.
28. Anantharaman, T. R., *The Rustless Wonder – A Study of the Delhi Iron Pillar*, Vigyan Prasar, New Delhi, 1997.
29. Balasubramaniam, R., *Indian J. Hist. Sci.*, 2002 (in press).
30. Ramesh Kumar, A. V. and Balasubramaniam, R., *Corros. Sci.*, 1998, **40**, 1169–1178.
31. Dillmann, P., Balasubramaniam, R. and Beranger, G., *ibid*, 2002, **44**, 2231–2242.
32. Kumar, V. and Balasubramaniam, R., *Int. J. Met., Mater. Process.*, 2002 (in press).
33. Stratmann, M. and Hoffman, K., *Corros. Sci.*, 1989, **29**, 1329–1352.
34. Puri, V., Balasubramaniam, R. and Ramesh Kumar, A. V., *Bull. Met. Mus.*, 1997, **28–II**, 1–10.
35. Tomoshov, N. D. and Chernova, G. P., *Passivity and Protection of Metals Against Corrosion*, Plenum Press, New York, 1967, pp. 151–180.


ACKNOWLEDGEMENTS. I acknowledge the co-operation of the Archaeological Survey of India in studies on the Delhi iron pillar.

Received 8 February 2002; revised accepted 19 April 2002